Collective excitations in adsorbed alkali-metal films: Critical analysis of photoyield and electron-energy-loss spectra for K on Al(111)

A. Liebsch,[1] Bong-Ok Kim,[2] and E. W. Plummer[2]
[1]*Institut für Festkörperforschung, Forschungszentrum Jülich, 52425 Jülich, Germany*
[2]*Department of Physics, University of Tennessee, Knoxville, Tennessee 37996*
and Solid State Division, Oak Ridge National Laboratory, Oak Ridge, Tennessee 37831-6057
(Received 1 June 2000; published 13 March 2001)

Photoyield and electron-energy-loss measurements were combined to elucidate the nature of the collective electronic modes of thin K films on Al(111). Various kinds of overlayer modes are observed whose frequency depends on coverage and parallel momentum. While photoemission is limited to the long-wavelength limit, electron-energy-loss spectroscopy provides information on the full $q_\parallel$ dispersion. Surprisingly, the loss frequencies measured at $q_\parallel=0$ differ appreciably from those observed in the photoyield spectra. They also exhibit a qualitatively different dependence on coverage. Calculations based on the time-dependent density-functional approach are carried out for both spectroscopies with the aim of analyzing the excitation spectra, in particular, the frequencies and relative intensities of overlayer modes as a function of coverage. We argue that for a consistent interpretation of photoyield and electron-energy-loss spectra it is crucial to account for the nonanalytic dispersion of the modes and their spectral weights at small $q_\parallel$ and for the finite angular resolution of the detector. The apparent discrepancies between the two spectroscopies are then resolved and the observed dispersions are in agreement with the density-functional predictions.

DOI: 10.1103/PhysRevB.63.125416 PACS number(s): 79.20.Kz, 79.60.Dp, 73.20.At

I. INTRODUCTION

The electronic excitations in thin metallic overlayers have attracted interest for nearly three decades because of the wide range of available electron densities and film thicknesses. Adsorbed alkali-metal films are important because of phenomena such as large work function changes, surface reconstruction, catalytic promotion, and metal–insulator transitions.[1,2] Despite the many studies that have been carried out so far, the understanding of adsorbate-induced collective modes is incomplete. In particular, the spectra obtained using different standard surface spectroscopies have never been compared on the same sample under identical surface conditions. This situation is quite different from the one on clean simple metals[3] where the $q_\parallel$ dispersion of the monopole and multipole surface-plasmon modes is now rather well understood for a variety of systems.[4–8] Moreover, the relationship between the multipole mode observed in electron-energy-loss spectroscopy (EELS) and the local-field enhancement[9–12] detected in photoyield spectra of simple metals[13,14] is well established.

For clean metal surfaces, the frequency of the ordinary surface plasmon in the long-wavelength limit ($q_\parallel=0$) is a bulk property: it is determined by the condition $\epsilon(\omega)=-1$, where $\epsilon(\omega)$ is the bulk dielectric function. No such simple relation exists for adsorbed films. In fact, the overlayer modes should be viewed as intrinsic surface excitations of the adsorbate–substrate system. Their frequencies and weights depend, even in the small $q_\parallel$ limit, on the details of the electronic properties of the system and its dynamical response to external fields.

Previous photoemission measurements on alkali metal overlayers focused primarily on the detection of quantum well states.[15] Only recently, photoyield data revealing various collective excitations of adsorbed alkali metals have been reported.[16,17] Although extensive EELS measurements on adsorbed alkali-metal films were performed in the past, their analysis is inconclusive because of the coverage dependence of spectral features, the large intrinsic peak widths, and the finite angular resolution of the detector.[18–23] As a result, the unambiguous identification of electronic surface excitations induced by metallic adsorbates and the evolution of these modes with increasing coverage to those of the semi-infinite metal, are still lacking.

In the present paper we report a systematic study of the collective surface excitations of K layers adsorbed on Al(111).[24] The coverage ranges from submonolayers to very thick films whose excitations resemble those of semi-infinite K. The key aspect of this paper is that we use both photon and electron spectroscopies since either one of them is insufficient to map out the complete range of excitations. While for photons only the long-wavelength region is accessible, in principle EELS covers the full dispersion between the long- and short-wavelength regions ($0\leqslant q_\parallel\leqslant 0.4$ Å^{-1}). In the $q_\parallel=0$ limit both spectroscopies should yield consistent spectral data.

One of the important results of our paper is the finding that there is no simple relationship between the adsorbate modes observed in photoyield spectra and the $q_\parallel=0$ peak positions detected using EELS: At no coverage do the electron-excited loss frequencies match the photon-generated modes. Moreover, whereas the photon-excited mode frequencies are virtually independent of coverage, the electron-excited modes vary greatly with overlayer thickness. These observations suggest that the identification of the modes observed in EELS is far from obvious and that a careful analysis is required, even in the small $q_\parallel$ limit.

To resolve these inconsistencies it is necessary to account

for the nonanalytic cusplike behavior of the dispersion and spectral weight of the overlayer modes at small $q_\parallel$. This behavior, combined with the finite aperture of the detector, leads to a redshift of the electron-excited modes by several tenths of an eV. The magnitude of this shift depends strongly on coverage. It is therefore in practice impossible using EELS to accurately determine the dispersion of overlayer modes in the small $q_\parallel$ region. Since this effective redshift is absent in the case of photoexcitation, significant *apparent* discrepancies between both spectroscopies arise.

This fundamental limitation of EELS had been overlooked in previous work and makes the interpretation of surface loss spectra considerably more subtle than had been assumed so far. As we show below, by properly accounting (i) for the detailed dispersion of the overlayer modes and their intensities at small $q_\parallel$ and (ii) for the influence of the finite detector aperture we are able to reconcile electron-energy-loss and photoyield spectra. In addition, these experimental observations are then in agreement with theoretical predictions.

According to the local optics model,[25] there exists only one overlayer mode, dispersing from the alkali-metal volume plasma frequency ω_p at small $q_\parallel$ towards the surface plasma frequency $\omega_s=\omega_p/\sqrt{2}$ at large $q_\parallel$. The coverage dependence of this mode is governed by the coupling factor $e^{-2q_\parallel a}$ (a is the adsorbate thickness), so that with increasing coverage the transition from ω_p to ω_s occurs at progressively smaller values of $q_\parallel \sim 1/a$. In the case of K, $\omega_p \approx 3.75$ eV and $\omega_s \approx 2.65$ eV; both frequencies lie far below the collective modes of the Al substrate ($\Omega_p \approx 15$ eV and $\Omega_s \approx 10.6$ eV).

Accounting for quantum-mechanical effects, i.e., the smoothness of the electronic density at the overlayer interfaces and the nonlocality of the dynamical response to the external field, calculations based on the time-dependent density-functional approach reveal a considerably more complex picture.[26]

The excitation spectra of alkali-metal adlayers comprise essentially four types of collective modes: monopole and multipole surface plasmons, bulklike overlayer plasmons, and the threshold excitation. The latter mode corresponds to $\hbar\omega \approx \Phi$, where Φ is the work function. The frequency of the multipole surface plasmon is approximately $\omega_m \approx 0.8\omega_p$. The frequencies and spectral weights of these modes in general depend on $q_\parallel$ and on coverage c. In addition, there are adsorbate-substrate interface modes at higher frequencies. The overlayer modes are broadened via electron-hole pair excitations and they can hybridize with one another. Moreover, because of different selection rules, the adsorbate modes couple differently to incident light and electrons.

Three coverage regions can be identified that exhibit qualitatively different excitation spectra:

(1) In the submonolayer regime, the main spectral feature is the threshold excitation caused by transitions from states near the Fermi energy to the vacuum level. Thus, for $c<1/2$, the spectra reveal a weak maximum near the work function Φ. As the coverage approaches one monolayer, the excitation frequency rapidly increases, but genuine overlayer surface plasmons are not yet formed.

(2) At a coverage of two monolayers, two collective modes appear: At $q_\parallel=0$, they correspond to the bulklike overlayer plasmon close to ω_p and the dipolar surface plasmon at ω_m. At finite $q_\parallel$, these modes undergo a transition towards the multipole and monopole surface plasmons of the alkali metal, respectively. As we discuss below, this transition involves the formation of a hybridization gap in the excitation spectrum.

(3) At even higher coverages, the frequencies of the $q_\parallel=0$ modes remain unchanged, while at finite $q_\parallel$ they disperse more and more rapidly towards the collective modes of the clean alkali-metal surface.

The outline of this paper is as follows. In Sec. II, the details of the experimental measurements are discussed. Section III describes the time-dependent density-functional approach for substrate-adsorbate systems and the overall behavior of induced charge densities and dynamical potentials. Section IV focuses on the analysis of the photoyield spectra. Section V discusses the EELS results and their relation to the yield data. Section VI contains some remarks on previous work. A summary is given in Sec. VII.

II. EXPERIMENT

The electron-energy-loss spectra were measured using a LH-22 angle-resolved electron energy-loss spectrometer mounted in a standard UHV chamber operated at a pressure of 4×10^{-11} Torr. The energy and angle of the incident electron beam were 15 eV and 60°.

The photoyield spectra were measured for 2–6 eV monochromatic light using the 150 W Xe lamp with 1/4m Seya–Namioka type monochromator. To check the quality of the film, photoyield for the *p*- and *s*-polarized light (Y_p, Y_s) were measured for each K film. The polished Al(111) sample was cleaned through routine Ne^+ sputtering and annealing. The cleanliness was checked by LEED and EELS. The K films were deposited from a K SAES getter source onto a clean Al(111) substrate cooled to 110 K. All spectra were measured at 110 K sample temperature. The surface roughness of the films was checked via the EELS angular resolution and the ratio Y_s/Y_p. The angle resolution was about 2°. Typically, we find that Y_s/Y_p is less than 2.5%. The origin of Y_s is bulk photoemission and surface photoemission with momentum gained from surface roughness. The main source of Y_p is surface photoemission with momentum gained via the surface barrier potential. The small values of Y_s/Y_p mean that our K films are smooth enough to detect photoemission caused by the large local field near the surface. The thickness of the films was calibrated by the work function measurements, thermal desorption spectra, and deposition time. The desorption of the $\sqrt{3}$ structure gives a peak near 150 to 220 °C, while the desorption of the higher coverage film gives another peak near 4 to 60 °C. Since the completion of the $\sqrt{3}$ structure corresponds to $\theta_K=0.33$, the film thickness can be calculated from the ratio of the two peak areas. $\theta_K=1$ refers to the underlying Al(111) structure. The coverage $c=1$ corresponding to the completion of the first K layer, has been reported as $\theta_K=0.45$ in other studies.[21,22]

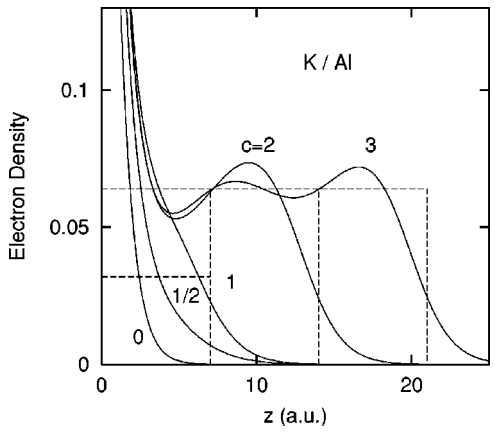

FIG. 1. Equilibrium electron-density profiles for K on Al at several coverages *c*. The positive background is indicated by the dashed lines. All curves are normalized to the bulk density.

III. THEORY

Since various theoretical aspects of the present paper have been discussed previously (see Ref. 3 and references herein), we give here only a brief outline of the important steps. The ground-state electronic properties of the K/Al adsorption system are treated within the jellium model and the local-density approximation (LDA).[27] For coverages up to three monolayers, convergence of the ground-state electron density is readily achieved. The one-electron potential near the center of the K film is then flat with a value equal to the asymptotic potential of semi-infinite K. Also, the work function for $c=3$ corresponds to that of semi-infinite K. For larger coverages we therefore cut the $c=3$ potential at the midpoint of the adsorbate slab and shift the surface barrier towards the vacuum. Equilibrium electron-densities higher coverages can then be readily evaluated. Of course, thicker films require a progressively finer grid of electron momenta.

Figure 1 illustrates ground-state densities for coverages up to three monolayers. The positive ionic background of the overlayer lies in the range $0 \leqslant z \leqslant a$. The substrate occupies the half-space $z \leqslant 0$. Only for $c \geqslant 2$ can the K/Al and K/vacuum interfaces be identified. At lower coverages, the K valence density merely amplifies the tail of the substrate density distribution. In view of these distributions it is to be expected that the electronic excitation spectra in the ranges $c<2$ and $c \geqslant 2$ will be qualitatively different.

To determine the dynamical response to the incident photons and electrons, we employ the adiabatic version of the time-dependent local-density approach (TDLDA),[28] i.e., exchange-correlation contributions to the effective local potential are approximated using the exchange-correlation potential of the ground state. Since dynamical corrections in the bulk appear at much higher frequencies (at about twice the volume plasma frequency according to present theories[29]), the adiabatic approximation is presumably adequate. At interfaces, dynamical corrections could play a role at lower frequencies than in the bulk due to excitation of surface plasmons and the intrinsically stronger coupling to electron-hole pairs. According to the rather large amount of evidence available so far,[3] however, such corrections apparently are not very important.

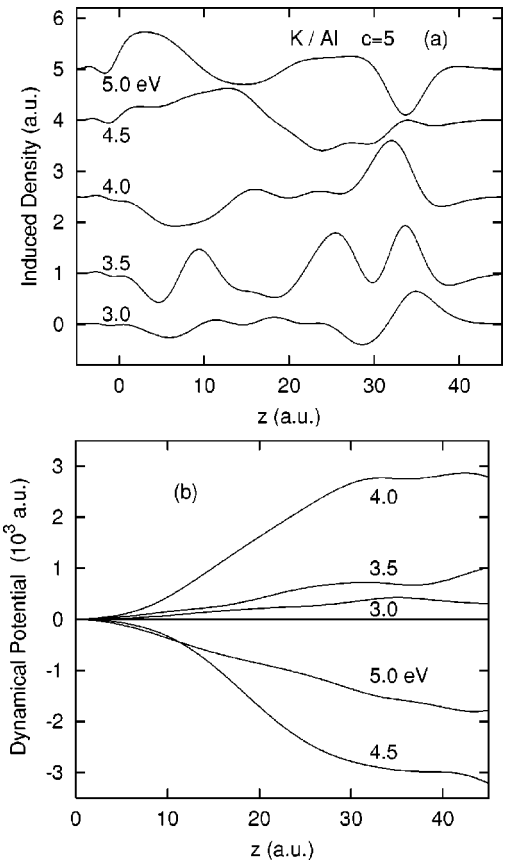

FIG. 2. The real part of (a) induced density $n_1(z,q_\parallel,\omega)$ and (b) dynamical potential $\phi_{\rm scf}(z,q_\parallel,\omega)$ for K on Al ($c=5$) at various photon energies, calculated within the TDLDA ($q_\parallel=0$). The overlayer is located between 0 and 35 a.u. The densities are vertically displaced for clarity.

Comparisons with excitation spectra obtained for fully three-dimensional overlayers employing nonlocal pseudopotentials[30] suggest that for alkali metals such as Na and K, the adsorbate-substrate jellium model gives an excellent representation of spectral features. Deviations induced by interband transitions appear, however, for systems involving stronger pseudopotentials such as Li.[8]

With the aid of the dynamical response calculations we obtain the frequency dependent local potential $\phi_{\rm scf}(z,q_\parallel,\omega)$ and induced electron density $n_1(z,q_\parallel,\omega)$. Because of the long range of the Coulomb potential, the $q_\parallel=0$ limit requires a computationally more sophisticated treatment than the case $q_\parallel>0$ where all fields and densities exhibit an overall decay towards the interior given by $e^{q_\parallel z}$. Nevertheless, at small $q_\parallel$ both schemes yield consistent excitation spectra.[3]

Figure 2 shows induced electronic densities and dynamical potentials for five monolayers of K on Al in the $q_\parallel=0$ limit. The frequencies span the range from below the K multipole surface plasmon to above the K bulklike overlayer plasmon. Up to about ω_m, the density is concentrated near the K/vacuum interface due to efficient screening, while near ω_p the fluctuating density extends across the entire K slab. The densities exhibit various short- and long-range dynami-

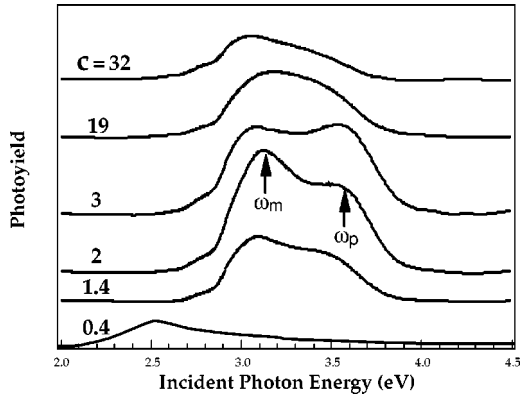

FIG. 3. Measured *p*-polarized photoyield spectra of thin K films adsorbed on Al(111). The coverage ranges from about $\theta_K = 0.23$ ($c = 0.5$) to $\theta_K = 14.5$ ($c = 32$). ω_m denotes the K multipole surface plasmon and ω_p the bulklike overlayer plasmon.

cal Friedel oscillations.[31] In contrast, the potentials are much smoother since the main contribution arises from Coulomb integrals over the induced densities. They are essentially linear functions of z (corresponding to nearly constant electric field within the overlayer) and become negligibly small at the K/Al interface.[32]

In the following section excitation spectra derived from fluctuating densities such as those shown in Fig. 2 will be compared to measured photoyield spectra. Analogous distributions obtained at finite $q_\parallel$ are used to derive the corresponding energy-loss spectra for incident electrons, which are the topic of Sec. V.

IV. SURFACE PHOTOYIELD SPECTRA

In this section we discuss the $q_\parallel = 0$ adsorbate-induced excitations, which can be studied most directly using incident photons. Figure 3 shows measured photoyield spectra for K on Al(111) at coverages ranging from $c = 0.5$ to $c = 32$. The spectra exhibit two spectral features near about 3.1 and 3.6 eV independently of coverage. They correspond to the K multipole surface plasmon and bulklike overlayer plasmon, respectively. The frequency of the multipole mode agrees well with the local-field enhancement observed in photoyield spectra of clean K.[13] The frequency of the upper peak lies slightly below the K volume plasmon observed in optical data, $\omega_p = 3.75$ eV. We note here that both modes lie well above the K monopole surface plasmon seen in EELS spectra of thick films ($\omega_s = 2.61$ eV; see below and Refs. 4 and 5).

In contrast to the coverage independent mode frequencies, the relative intensities vary strongly with coverage: near one monolayer and at large coverages the multipole peak is more intense, while at intermediate coverages the bulklike feature dominates. Below one monolayer coverage a shift of spectral weight to lower frequencies is observed.

These results are in good agreement with the $q_\parallel = 0$ overlayer modes predicted by the TDLDA[26] and with analogous photoyield measurements for K and Na on Al by Barman *et al.*[17] Figure 4 shows the theoretical spectra for K on Al for several coverages. Plotted is the function $\mathrm{Im}\, d_\perp(\omega)$, which is

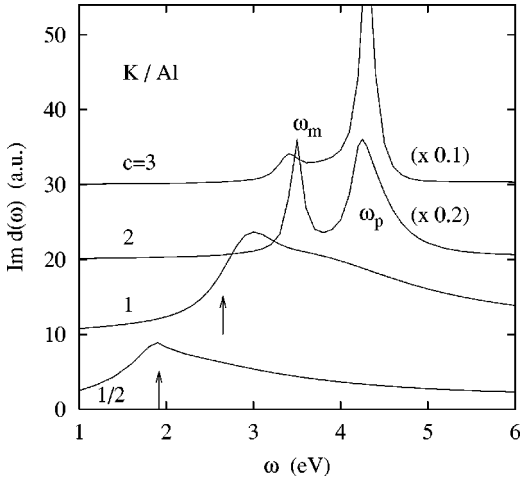

FIG. 4. Excitation spectra for K on Al at various coverages, calculated within the TDLDA ($q_\parallel = 0$). ω_m and ω_p are the theoretical multipole surface and volume plasma frequencies of K, respectively. The arrows denote the work functions for $c = 1/2$ and $c = 1$.

proportional to the photoyield (see below). Here, $d_\perp(\omega)$ defines the centroid of the surface screening density $n_1(z, q_\parallel = 0, \omega)$. Since these calculations do not include the effect of core polarization, the mode frequencies lie about 10% higher than the measured frequencies. For $r_s = 5$ one has $\omega_p = 4.21$ eV, while optical data give 3.75 eV. Accordingly, the calculated multipole frequency $\omega_m = 3.45$ eV should be scaled down to about 3.1 eV, which coincides with the measured multipole frequency shown in Fig. 3.

The physical reason for the existence of collective modes near ω_m and ω_p is that, for $c \geqslant 2$, the adsorbate exhibits a sufficiently wide region of nearly constant electron density, so that the adsorbate-substrate and adsorbate-vacuum interfaces are well separated (see Fig. 1). At $c \approx 1$, the electronic density within the overlayer is no longer plateaulike and the interfaces are not well defined. The peaks near ω_p and ω_m then become very broad and overlap. According to Fig. 4, the spectrum reveals only one feature with strongly mixed multipole and bulklike weight. Its maximum lies slightly below ω_m. This shift towards lower frequencies is also observed experimentally.

Below one monolayer, the ground-state density profile in the overlayer region merely enhances the tail of the substrate density (see Fig. 1). The TDLDA calculations indicate that the K multipole mode then also ceases to exist. Instead, the so-called threshold excitation near $\hbar\omega \approx \Phi$ appears. The yield measurement for $c = 0.5$ reveals indeed a strong suppression of spectral weight in the range of the overlayer collective modes, and a broad maximum near 2.5 eV, which qualitatively agrees with the theoretical results.

Towards larger coverages, the data shown in Fig. 3 indicate that the weight near ω_p diminishes. This is to be expected since for very thick overlayers the yield is given by[9,33]

$$Y(\omega) \sim (1 - \omega^2/\omega_p^2)\,\mathrm{Im}\, d_\perp(\omega). \tag{1}$$

The prefactor in this expression is related to the asymptotic internal field. The surface photoyield vanishes at the bulk

plasma frequency since a photoelectron emitted near the surface does not couple to a bulk mode of infinite wavelength. At low coverages ω_p corresponds to the substrate bulk plasma frequency Ω_p, whereas for thick overlayers, ω_p is the K volume plasma frequency. Thus, with increasing coverage, the peak near ω_p transforms into a minimum. This minimum had been observed previously in yield data on several simple metals.[13,14]

The intensity of the multipole mode also diminishes with increasing coverage because of the changing nature of the Fresnel field: The prefactor $(1-\omega^2/\omega_p^2)$ decreases from $1-(3.1/15.2)^2=0.96$ for K on Al to $1-(3.1/3.75)^2=0.32$ for semi-infinite K. For a similar reason, $\mathrm{Im}\, d_\perp(\omega_m)$ is smaller for clean K than for K on Al. This may be seen by expressing $d_\perp(\omega_m)$ as $p(\omega)/\sigma(\omega)$, where $\sigma=(\varepsilon-1)/(\varepsilon+1)=1/(1-2\omega^2/\omega_p^2)$ is the total weight of the dynamical charge and p its dipole moment. While p is roughly independent of coverage, $1/\sigma$ decreases from $1-2(3.1/15.2)^2=0.92$ for K on Al to $|1-2(3.1/3.75)^2|=0.37$ for semi-infinite K. Thus, both factors contributing to the yield at the multipole frequency diminish with coverage, in agreement with the spectra shown in Fig. 3.

It is at first sight surprising that, already for a coverage of two monolayers, the frequency of the bulklike overlayer mode agrees quite well with that of the nominal bulk plasmon of K. According to the TDLDA results, $\omega_p \approx 4.3$ eV for $c=2$–3 compared to $\omega_p(K)=4.2$ eV. Apparently, several competing factors lead to a near cancellation. While the finite overlayer thickness and the spillover of charge at the K/Al interface give a blueshift, the spillout of charge at the K/vacuum interface and the diffuseness of both interfaces should cause a redshift. We can estimate the confinement-induced blueshift by assuming the adsorbate thickness $a \approx 14$ a.u. for $c=2$ to correspond to half a plasmon wavelength. Bulk loss measurements[34] indicate that the K volume plasma frequency at $q=\pi/a$ lies 0.2 eV above the $q=0$ value. At $c=4$ this shift is only 0.05 eV.

Another interesting point is that the adiabatic TDLDA gives an excellent prediction of the multipole plasma frequency. Assuming the same relation for K as for jellium at $r_s=5$, i.e., $\omega_m=0.82\omega_p$, we have $\omega_m=0.82\times 3.75=3.08$ eV, which agrees with the measured value.[35] Omitting the exchange-correlation contribution from the dynamical potential, i.e., treating the response within the RPA, gives instead $\omega_m=0.89\,\omega_p=3.34$ eV. This value is much higher than the observed multipole frequency. The origin of this blueshift is the more repulsive bare Coulomb interaction, which effectively makes the density profile less polarizable than in the TDLDA. The good agreement between measured and predicted multipole frequencies also suggests that dynamical corrections to the local potential are small. The bulklike overlayer mode is less affected by the treatment of exchange-correlation terms since these stem primarily from the interfaces where the ground-state density is varying. Thus, this mode is essentially governed by the bare Coulomb interaction.

We point out that the measured overlayer spectral peaks are much broader than the calculated ones shown in Fig. 4.

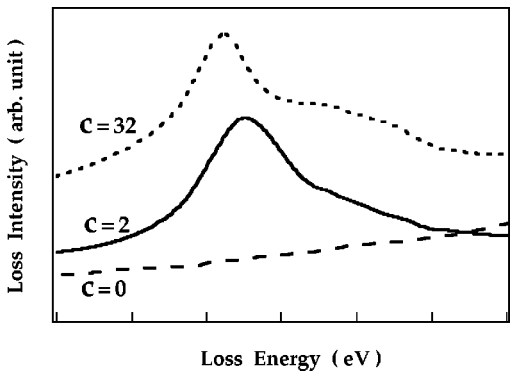

FIG. 5. Measured electron-energy-loss spectra at $q_\parallel=0$ for K on Al(111). Solid curve: $c\approx 2$, dotted curve: $c\approx 32$. The clean Al loss spectrum is indicated by the dashed curve.

Since the calculations do not include lifetime broadening nor damping due to interband transitions, they underestimate the peak widths. Also, although the samples appear to be rather smooth ($Y_p \gg Y_s$), regions of different adsorbate thickness cannot be excluded.

We close this section by discussing briefly the possibility of observing higher bulklike overlayer plasmons in photoyield spectra. Since these modes correspond to surface excitations of the adsorbate-substrate system, observation via incident light is in principle feasible. Anderegg *et al.*[36] had detected such modes many years ago in yield spectra for thick K films grown on quartz. The coupling to these modes was rather weak and only differentiation of the yield with respect to the light wavelength revealed fine structure that could be associated with standing waves. Surprisingly, it is now known that the measured bulk plasmon dispersion of K (Ref. 34) is not quadratic up to the large wave vectors assumed by Anderegg *et al.* The present yield data do not exhibit any evidence of bulklike plasmon modes beyond the lowest-order oscillation. This might be related to the fact that the Al substrate is not as smooth as the quartz substrate, and to the larger damping of K plasmon modes due to electron-hole pair creation at the K/Al interface.

In sum, the K-induced electronic excitations observed in photoyield spectra agree well with TDLDA predictions. Their frequencies are nearly independent of coverage, whereas their relative intensities change strongly. In particular, with increasing coverage the bulklike peak at ω_p turns into a minimum consistent with observations for clean alkali-metal surfaces.

V. ELECTRON-ENERGY-LOSS SPECTRA

We now turn to the adsorbate-induced excitations observed in electron energy-loss spectra, in particular, their dispersion with parallel wave vector. Consider first the loss spectra for $q_\parallel=0$, which are shown in Fig. 5 for several coverages. Clean Al exhibits only a smooth background in the 2–6 eV range. For $c=2$, the K overlayer induces a main peak at 2.76 eV with a weak shoulder extending from 3.2 to 4.0 eV. For $c=32$, the main peak has shifted down to $\omega_s=2.61$ eV and the high-frequency shoulder is more pro-

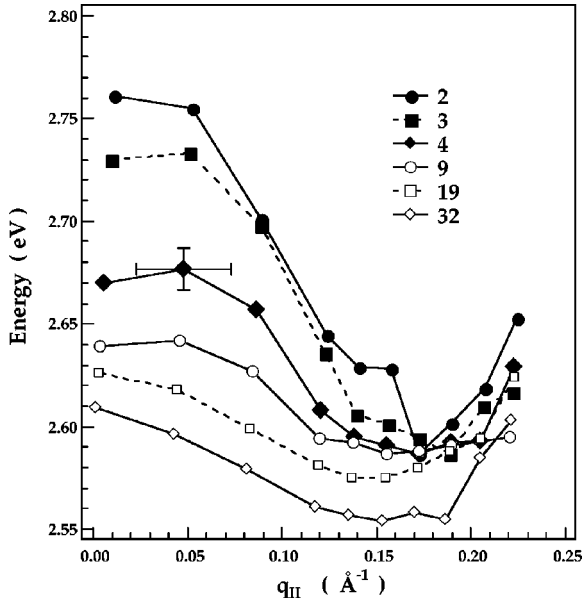

FIG. 6. Measured momentum dispersion of main collective mode of K on Al(111) for coverages $\theta_K = 0.96, \ldots, 14.5$ ($c = 2.1, \ldots, 32$).

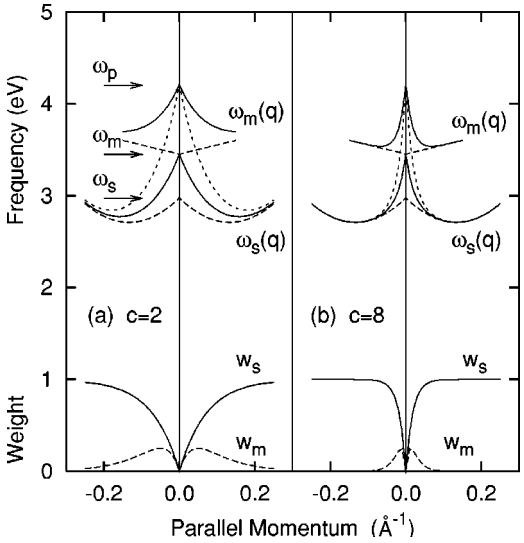

FIG. 7. Dispersion of collective electronic excitations for K on Al (upper-solid curves). Dashed curves: surface modes of semi-infinite K. Dotted curves: local-optics mode dispersing from ω_p to $\omega_s(q)$. Lower curves: spectral weight of adsorbate-induced modes. (a) $c=2$; (b) $c=8$.

nounced. In fact, this shoulder appears to consist of separate spectral features near 3.25 and 3.75 eV.[37]

Evidently, there is no simple relationship between the adsorbate modes observed in the yield spectra in Fig. 3 and the $q_\parallel = 0$ peak positions detected using EELS. The spectra differ in two fundamental ways: First, the photon-generated mode frequencies ω_m and ω_p are practically independent of coverage, whereas the electron-excited modes vary strongly with overlayer thickness. Second, at no coverage do the electron-excited loss frequencies match those generated via photons. These discrepancies indicate that the identification of the modes observed in EELS is nontrivial, even in the $q_\parallel = 0$ limit. It is to be expected that similar difficulties arise at finite $q_\parallel$.

Figure 6 shows the dispersion of the main K-induced mode for various coverages. To determine the mode frequencies, each loss peak was fitted to a Lorentzian after removal of a smooth background similar to the clean Al loss spectrum. The dispersion of the upper spectral feature is difficult to determine because of its large width. This shoulder appeared always on the high-frequency side of the main peak, i.e., a crossing of these two overlayer spectral features as a function of $q_\parallel$ can be excluded.

In the following we show that the EELS data are in fact compatible with the photoyield spectra and that both are well represented by the TDLDA predictions. The key point is that the peak positions observed in EELS do *not* correspond to the actual mode frequencies. Instead, because of the finite detector aperture and the negative dispersions with $q_\parallel$, they represent *apparent* frequencies that lie several tenths of an eV *below* the *true* mode frequencies. This mismatch becomes particularly severe near $q_\parallel = 0$ and for increasing overlayer thickness.

A. Nonanalyticity of overlayer modes

To illustrate the *nonanalytical*, cusplike dispersion of the frequency and spectral weight of the overlayer modes at small $q_\parallel$, we show in Fig. 7 the dispersion of the K-induced modes predicted by the TDLDA.[26,38] The mode frequencies correspond to the positions of spectral peaks obtained in dynamical response calculations carried out at finite $q_\parallel$. [As pointed out above, these calculations do not include the effect of core polarization. In order to compare them with the experimental data, all frequencies should therefore be scaled down by about 10%.] According to these results, two K-induced modes exist that disperse like $\omega_{ms}(q_\parallel) = \omega_m(0) \rightarrow \omega_s(q_\parallel)$ and $\omega_{pm}(q_\parallel) = \omega_p(0) \rightarrow \omega_m(q_\parallel)$. Before discussing the origin of these dispersions, we point out that in the $q_\parallel = 0$ limit, these modes are in fact identical to the ones found in the photon response calculations. Thus, for $c=2$ one should observe modes at ω_m and ω_p just as in the photoyield spectra shown in Figs. 3 and 4. This statement ignores the $q_\parallel$ dispersion of the frequency and spectral weight of these modes and assumes perfect analyzer resolution. If we include these aspects, however, the picture changes considerably.

In the present experiment the angular aperture of the spectrometer amounts to about $\Delta q_\parallel = 0.05$ Å^{-1}. Thus, even if the analyzer is nominally set at $q_\parallel = 0$, one integrates an approximately circular area up to $q_\parallel \leqslant 0.025$ Å^{-1}. Because of the negative dispersion, this integration gives rise to an apparent redshift of the mode frequency. Obviously, the true $q_\parallel = 0$ mode contributes less to the observed spectral intensity than those at finite $q_\parallel$, in particular, since its weight at $q_\parallel = 0$ vanishes, as illustrated in the lower part of Fig. 7(a). Thus, for the proper analysis of loss spectra, it is crucial to account also for the q dependence of peak intensities.

The vanishing strength of the overlayer modes in the $q_\parallel = 0$ limit may be understood as follows. Within the dipole

approximation, the loss spectrum at small $q_\parallel$ observable in EELS is determined by the surface loss function[39]

$$\mathrm{Im}\, g(q_\parallel,\omega) = \mathrm{Im} \int dz\, e^{q_\parallel z} n_1(z,q_\parallel,\omega) \rightarrow \mathrm{Im} \frac{\epsilon(\omega)-1}{\epsilon(\omega)+1}\left[1+2q_\parallel d_\perp(\omega)\frac{\epsilon(\omega)}{\epsilon(\omega)+1}\right], \quad (2)$$

where $\epsilon(\omega)$ is the bulk dielectric function of the substrate. (We neglect here small contributions from $d_\parallel$.) Thus, at $q_\parallel = 0$, the only collective surface mode visible is determined by the condition $\epsilon(\omega) = -1$, corresponding to the substrate surface plasmon at Ω_s. At small $q_\parallel$, there is no mode at ω_s associated with the adsorbate monopole surface plasmon. Surface photoyield spectra, on the other hand, are governed by the quantity $\mathrm{Im}\, d_\perp(\omega)$ as indicated in Eq. (1). Equation (2) then implies that the overlayer modes at ω_p and ω_m that are observed using photons [i.e., the peaks in $\mathrm{Im}\, d_\perp(\omega)$] have vanishing weight in electron-loss spectra at $q_\parallel = 0$ and that their weight increases linearly with $q_\parallel$. Thus, averaging over $q_\parallel$ within detector resolution implies sampling modes at finite $q_\parallel$ because of their finite spectral weight. We conclude, therefore, that the electron-excited modes are in fact compatible with the photon-generated excitations, but the *effective* peak positions observed in EELS are redshifted. As we show below, this redshift depends strongly on coverage. Of course, for incident photons there is no redshift since the excitation occurs in the $q_\parallel = 0$ limit and the finite detector aperture merely implies collection of a finite range of momenta of the outgoing electron.

B. Hybridization gap in overlayer spectrum

To understand the coverage dependence of the *effective* peak positions observed in EELS, let us return to Fig. 7(a) and develop a simple physical picture for the theoretical dispersion of the overlayer modes found within the TDLDA. Consider first the local optics model.[25] In this case, there exists only one overlayer excitation dispersing from ω_p towards ω_s (see dotted curve). In fact, the frequency of this mode is roughly given by $\omega_{ps}(q_\parallel) \approx \omega_p e^{-2q_\parallel a} + \omega_s(1 - e^{-2q_\parallel a})$. Its weight increases approximately like $w_{ps}(q_\parallel) \approx 1 - e^{-2q_\parallel a}$. As before, a is the overlayer thickness. Quantum-mechanical effects not only modify the dispersion of this mode, but also give rise to the multipole surface plasmon, which is a response property of the adsorbate-vacuum interface. The dispersion of $\omega_m(q_\parallel)$ should therefore be positive just as on the clean alkali metal (see upper dashed line). Within this simple picture we have two modes dispersing like

$$\omega_{ps}(q_\parallel) = \omega_p(0) \rightarrow \omega_s(q_\parallel), \quad (3)$$

$$\omega_{mm}(q_\parallel) = \omega_m(0) \rightarrow \omega_m(q_\parallel). \quad (4)$$

Now, since $\omega_m(0) \approx 0.8\omega_p$ and $\omega_s \approx 0.7\omega_p$, it is evident that the principal electrostatic slab mode $\omega_{ps}(q_\parallel)$ and the multipole surface plasmon $\omega_{mm}(q_\parallel)$ cross unless both modes may couple via common excitation mechanisms. As pointed out above, the overlayer-induced modes are surface modes of the adsorbate-substrate system. Thus both couple to electron-hole excitations. The TDLDA calculations reflect this coupling since they show that the mode crossing is avoided by opening a *hybridization gap*. We therefore arrive at two new noncrossing modes[26]

$$\omega_{pm}(q_\parallel) = \omega_p(0) \rightarrow \omega_m(q_\parallel), \quad (5)$$

$$\omega_{ms}(q_\parallel) = \omega_m(0) \rightarrow \omega_s(q_\parallel). \quad (6)$$

These results also demonstrate that only at $q_\parallel = 0$ and $q_\parallel \gg 1/a$ the overlayer modes have pure monopole, multipole, or bulklike nature. At intermediate $q_\parallel$, the modes represent mixtures of these elementary excitations. Because of the finite detector aperture, an effective mode mixing occurs even in the $q_\parallel = 0$ limit.

C. Coverage dependence of overlayer modes

Suppose now that we increase the overlayer thickness. Clearly, the main electrostatic slab mode disperses more rapidly from ω_p down towards ω_s (see above). The multipole mode, on the other hand, is a property of the adsorbate-vacuum interface and therefore independent of coverage. Thus, the avoided-crossing transition $\omega_m(0) \rightarrow \omega_s(q_\parallel)$ and $\omega_p(0) \rightarrow \omega_m(q_\parallel)$ must occur at progressively smaller $q_\parallel \sim 1/a$.[26,40] This behavior is indicated in Fig. 7(b) where we plot the dispersions of the mode frequencies and spectral weights for $c = 8$. Accounting again for the finite detector aperture, it is clear that the modes at $\omega_m(0)$ and $\omega_p(0)$ become less and less important and we recover the collective surface modes $\omega_s(q_\parallel)$ and $\omega_m(q_\parallel)$ of the semi-infinite alkali metal. Eventually, of course, the small-$q_\parallel$ region is dominated by retardation effects.

The above analysis shows that, while the mode frequencies observed in yield spectra are nearly independent of coverage, the peak positions detected in EELS represent *apparent* modes whose frequencies vary strongly with overlayer thickness, even in the nominal $q_\parallel = 0$ limit. In practice, it is therefore impossible using EELS to detect the true frequencies of the overlayer modes. Their nonanalytical behavior at $q_\parallel = 0$ and negative dispersion at finite $q_\parallel$ imply a coverage-dependent redshift. According to the experimental data shown in Figs. 3 and 5, the redshift of $\omega_m = 3.1$ eV at $q_\parallel = 0$ amounts to about 0.35 eV at $c = 2$ and 0.5 eV at $c = 32$. In the latter case, this mode has effectively become $\omega_s(0) = 2.6$ eV.

To verify that this picture is reasonable, let us estimate the film thickness at which the observed position of the main K loss peak at $q_\parallel = 0$ converges to the surface plasma frequency $\omega_s(0)$. Since the transition $\omega_m(0) \rightarrow \omega_s(q_\parallel)$ is complete when the coupling factor $e^{-2q_\parallel a}$ is small, we have $2q_\parallel a \approx 5$ or $a \approx 5/\Delta q_\parallel$, where $\Delta q_\parallel = 2q_\parallel \approx 0.05$ Å^{-1} is the detector aperture. Thus, $a \approx 100$ Å or $c \approx 30$ monolayers. This estimate agrees very well with the data shown in Fig. 5.

The redshift of ω_p at $q_\parallel = 0$ is more difficult to quantify because of the large width of the high-frequency shoulder observed in Fig. 5. It lies between 0.2 and 0.4 eV below the upper overlayer mode seen in the yield spectrum near $\omega_p(0)$.

This redshift is also the result of the finite detector aperture, the negative, nonanalytical dispersion of the overlayer mode, $\omega_p(0) \rightarrow \omega_m(q)$, and the vanishing spectral weight of this mode at $q_\parallel = 0$.

So far, we have discussed the dispersion of the frequencies of the overlayer modes. Let us now briefly comment on their intensities. According to the calculated loss spectra,[20,26] the lower adsorbate mode dispersing like $\omega_m(0) \rightarrow \omega_s(q_\parallel)$ is more intense than the upper mode $\omega_p(0) \rightarrow \omega_m(q_\parallel)$. This result is consistent with the measured loss data shown in Fig. 5 for $q_\parallel = 0$ and with analogous spectra at finite $q_\parallel$. Thus, as predicted by the TDLDA, we observe two overlayer modes that do not cross, confirming the existence of a hybridization gap in the adsorbate excitation spectrum. This gap is reminiscent of the gap between ω_s and ω_p in the dispersion of the surface-plasmon polariton. In the absence of retardation, the ordinary surface plasmon crosses the light line. Due to electromagnetic coupling, this crossing is avoided and a gap is opened in the polariton excitation spectrum.

D. Large-coverage limit

Interestingly, the high-frequency shoulder in the loss spectrum for $c = 32$ in Fig. 5 seems to consist of two spectral features at 3.3 and 3.7 eV. In fact, this spectral distribution is consistent with the one observed by Tsuei *et al.*[5] for very thick K films. Thus, at this large overlayer thickness ($a \approx 100$ Å) and for $q_\parallel = 0$, the main K mode $\omega_{ms}(q_\parallel) = \omega_m(0) \rightarrow \omega_s(q_\parallel)$ has converged towards $\omega_s(0)$ of clean K, the upper overlayer mode $\omega_{pm}(q_\parallel) = \omega_p(0) \rightarrow \omega_m(q_\parallel)$ has become $\omega_m(0)$, and, finally, excitation of a propagating bulk plasmon of semi-infinite K at $\omega_p \approx 3.7$ eV has become possible. These spectra indicate for the first time how the collective overlayer modes detected in EELS evolve with increasing coverage towards the collective surface excitations of clean semi-infinite alkali metals.

E. Less than two monolayers

The above discussion focused on the excitations for coverages of two or more monolayers. As pointed out in the preceding section, for $c = 1$ the adsorbate interfaces are no longer well defined and there is no plateau of roughly constant density. It seems plausible that such a density profile does not support the same modes as a semi-infinite alkali metal. For $q_\parallel = 0$, the broad spectral peak consists of strongly mixed multipole and bulk plasmon contributions. In addition, the TDLDA calculations show that at finite $q_\parallel$ this peak shifts to lower frequencies.[26] Unlike for $c \geq 2$ and on the semi-infinite surface, the $c = 1$ mode exhibits no minimum as a function of $q_\parallel$. Thus, although its frequency lies in the overall range of the monopole mode $\omega_s(q_\parallel)$ for $c > 2$, it is not meaningful to refer to the $c = 1$ spectral peak as true surface plasmon.

VI. RELATION TO PREVIOUS WORK

We point out that the TDLDA calculations and the loss data show that the initial slope of the main overlayer mode at small $q_\parallel$ is steeper than that of the clean surface monopole plasmon. This agrees with previous EELS measurements by Tsuei.[20,6] Also, for $q_\parallel > 0.15$ Å^{-1}, the main overlayer mode exhibits a positive dispersion. This observation is consistent with the early EELS data for K and Na on Ni by Andersson and Jostell.[18]

We also comment on recent EELS measurements for K on Ni(111) by Chiarello *et al.*[23] These authors claimed that ''contrary to theoretical predictions, at small $q_\parallel$ the excitation of the surface plasmon for two K layers is possible.'' A careful analysis, however, shows that the K/Ni data fully confirm the TDLDA results. In fact, for $c = 2$, the observed dispersion of the main K-induced loss is remarkably similar to the one shown in Fig. 5. At $q_\parallel = 0.05$ Å^{-1}, the main peak lies at 2.71 eV. (The data point at $q_\parallel = 0.02$ Å^{-1} and $\omega = 2.69$ eV lies significantly below the dispersion of all other points.) Extrapolation of the main dispersion to $q_\parallel = 0$ yields about 2.78 eV, i.e., distinctly above the actual $q_\parallel = 0$ monopole surface plasma frequency of clean K, $\omega_s(0) \approx 2.65$ eV. This finding is clear evidence of the fact that the main overlayer mode $\omega_{ms}(q_\parallel)$ disperses from $\omega_m(0) \approx 3.1$ eV towards $\omega_s(q_\parallel)$. At finite $q_\parallel$, therefore, the loss peak must be located at intermediate frequencies, just as observed. Moreover, the K/Ni spectra for $q_\parallel = 0.05$ Å^{-1} reveal a broad high-frequency shoulder near 3.4 eV, i.e., far above $\omega_m(0) = 3.1$ eV. The frequency of the observed shoulder confirms the dispersion of the upper overlayer mode $\omega_{pm}(q_\parallel) = \omega_p(0) \rightarrow \omega_m(q_\parallel)$ and the redshift caused by the finite aperture. As in the case of the present K/Al data, this weak feature remained always on the high-frequency side of the main peak.

Thus, the K/Ni spectra are in agreement with the TDLDA predictions, including the avoided crossing giving rise to the opening of the hybridization gap. It is, however, important to recall that at the ''small wave vector'' referred to by Chiarello *et al.*, i.e., at $q_\parallel = 0.05$ Å^{-1}, the overlayer modes already have dispersed down from the $q_\parallel = 0$ mode frequencies by several tenths of an eV. Moreover, even with the analyzer set at $q_\parallel = 0$, the peak positions lie significantly below the true $q_\parallel = 0$ mode frequencies observed in surface photoyield spectra. We conclude, therefore, that for $c = 2$, the electromagnetic fields are effectively screened within the alkali-metal overlayer, so that the nature of the substrate (Ni vs Al) has a minor influence on the dispersion of the collective modes. For about one monolayer, the K/Ni data reveal an appreciable redshift that is also compatible with earlier work[18,19] and with theoretical results for K on Al.[20,26]

It would be interesting to extend the EELS measurements on K/Ni to larger coverages. According to the present analysis, the lower K-induced collective mode at $q_\parallel = 0$ should then shift further down towards the clean K monopole plasma frequency $\omega_s(0) \approx 2.6$–2.7 eV. Similarly, the high-frequency shoulder near 3.4 eV should shift down towards $\omega_m(0) \approx 3.1$ eV. In addition, new spectral weight should appear near $\omega_p(0) \approx 3.75$ eV. In contrast, photoyield measurements on K/Ni beyond two monolayers should give rise to thickness-independent spectral peaks near $\omega_m(0) \approx 3.1$ eV and $\omega_p(0) \approx 3.6$–3.75 eV.

VII. SUMMARY

Using both EELS and surface photoemission, a systematic understanding of the collective electronic excitations in thin K films on Al(111) has been achieved. The data show that the measured spectra in the long-wavelength limit differ significantly for these two spectroscopies and that the mode frequencies exhibit a fundamentally different coverage dependence. These discrepancies can be understood by taking into account the nonanalyticity of the mode frequencies and spectral weights at $q_\parallel = 0$. Thus, in photoyield measurements two overlayer modes are found corresponding to the K multipole surface and bulklike overlayer plasmon. While their frequencies are nearly independent of coverage, the bulklike spectral peak turns into a minimum for very thick overlayers. In EELS, the $q_\parallel$ dependence of these modes is observed. The multipole surface and bulklike plasmons then disperse towards the monopole and multipole surface plasmons, respectively. A mode crossing is avoided by the opening of a hybridization gap in the excitation spectrum. A crucial point, however, is that in EELS the mode frequencies are redshifted by several tenths of an eV, because of the vanishing weight and cusplike dispersion at small $q_\parallel$. Once these effects are accounted for, the photoyield and EELS data are consistent with one another and with the dispersions predicted within the TDLDA.

ACKNOWLEDGMENTS

This work was funded by NSF DMR-9510132. Oak Ridge National Laboratory is managed by Lockheed Martin Energy Research Corp. for U.S. DOE under Contract No. DE-AC05-96OR22464

[1] T. Aruga and Y. Murata, Prog. Surf. Sci. **31**, 61 (1989).
[2] *Physics and Chemistry of Alkali Metal Adsorption*, edited by H. P. Bonzel, A. M. Bradshaw, and G. Ertl (Elsevier, Amsterdam, 1989).
[3] A. Liebsch, *Electronic Excitations at Metal Surfaces* (Plenum, New York, 1997).
[4] K.-D. Tsuei, E. W. Plummer, and P. J. Feibelman, Phys. Rev. Lett. **63**, 2256 (1989).
[5] K.-D. Tsuei, E. W. Plummer, A. Liebsch, K. Kempa, and P. Bakshi, Phys. Rev. Lett. **64**, 44 (1990); K.-D. Tsuei, E. W. Plummer, A. Liebsch, E. Pehlke, K. Kempa, and P. Bakshi, Surf. Sci. **247**, 302 (1991).
[6] K.-D. Tsuei, Ph.D. thesis, University of Pennsylvania, 1990.
[7] P. D. Sprunger, G. M. Watson, and E. W. Plummer, Surf. Sci. **269/270**, 551 (1992).
[8] H. Ishida and A. Liebsch, Phys. Rev. B **54**, 14 127 (1996).
[9] P. J. Feibelman, Prog. Surf. Sci. **12**, 287 (1982).
[10] K. Kempa and R. R. Gerhardts, Solid State Commun. **53**, 579 (1985).
[11] A. Liebsch, Phys. Rev. B **36**, 7378 (1987).
[12] K. Kempa and W. L. Schaich, Phys. Rev. B **37**, 6711 (1988).
[13] J. Monin and S. G. A. Boutry, Phys. Rev. B **9**, 1309 (1974).
[14] H. J. Levinson, E. W. Plummer, and P. J. Feibelman, Phys. Rev. Lett. **43**, 952 (1979).
[15] A. Carlsson, D. Claesson, S.-Å. Lindgren, and L. Walldén, Phys. Rev. Lett. **77**, 346 (1997), and references therein.
[16] I. N. Yakovkin, G. A. Katrych, A.T. Loburets, Y. S. Vedula, and A. G. Naumovets (unpublished); G. A. Katrych, N. V. Petrova, and I. N. Yakovkin, Ukr. Phy. J. **39**, 73 (1994).
[17] S. R. Barman, K. Horn, P. Häberle, H. Ishida, and A. Liebsch, Phys. Rev. B **57**, 6662 (1998).
[18] S. Andersson and U. Jostell, Surf. Sci. **46**, 625 (1974); Faraday Discuss. Chem. Soc. **60**, 255 (1975).
[19] D. Heskett, K. H. Frank, K. Horn, E. E. Koch, H. J. Freund, A. Baddorf, K. D. Tsuei, and E. W. Plummer, Phys. Rev. B **37**, 10 387 (1989), and references therein.
[20] J. A. Gaspar, A. G. Eguiluz, K. D. Tsuei, and E. W. Plummer, Phys. Rev. Lett. **67**, 2854 (1991).
[21] J. N. Andersen, E. Lundgren, R. Nyholm, and M. Qvarford, Surf. Sci. **289**, 307 (1993).
[22] H. Kondoh and H. Nozoye, Surf. Sci. **329**, 32 (1995).
[23] G. Chiarello, A. Cupolillo, A. Amoddeo, L. S. Caputi, L. Papagno, and E. Colavita, Phys. Rev. B **55**, 1376 (1997).
[24] B.-O. Kim, Ph.D. thesis, University of Pennsylvania, 1999.
[25] J. W. Gadzuk, Phys. Rev. B **1**, 1267 (1970).
[26] A. Liebsch, Phys. Rev. Lett. **67**, 2858 (1991).
[27] N. D. Lang, Phys. Rev. B **4**, 4234 (1971).
[28] A. Zangwill and P. Soven, Phys. Rev. A **21**, 1561 (1980).
[29] H. M. Böhm, S. Conti, and M. P. Tosi, J. Phys. CM **8**, 781 (1996); K. Sturm and A. Gusaraov, Phys. Rev. B (to be published); see also: E. K. U. Gross and W. Kohn, Phys. Rev. Lett. **55**, 2850 (1985); I. Iwamoto and E. K. U. Gross, Phys. Rev. B **35**, 3003 (1987).
[30] H. Ishida and A. Liebsch, Phys. Rev. B **45**, 6171 (1992).
[31] P. J. Feibelman, Phys. Rev. B **12**, 1319 (1975).
[32] The limited spatial extent of the dynamical potential can lead to quantum well behavior in the absence substrate-adsorbate potential barriers. See S. R. Barman, K. Horn, P. Häberle, and A. Liebsch (to be published).
[33] Note that $\mathrm{Im}\, d_\perp(\omega)$ accounts for the total surface absorption, i.e., for externally emitted electrons and those propagating to the back of the sample. Both processes exhibit the same resonances but may have appreciably different spectral weights. See J. T. Lee and W. L. Schaich, Phys. Rev. B **44**, 13 010 (1991); A. Liebsch, G. V. Benemanskaya, and M. N. Lapushkin, Surf. Sci. **302**, 303 (1994).
[34] A. Vom Felde, J. Sprösser-Prou, and J. Fink, Phys. Rev. B **40**, 10 181 (1989).
[35] Some uncertainty here arises from the measured bulklike plasma frequency. Because of the not fully controlled morphology of the evaporated overlayers, the frequency obtained from bulk optical data is presumably the correct reference value.
[36] M. Anderegg, B. Feuerbacher, and B. Fitton, Phys. Rev. Lett. **27**, 1127 (1971).
[37] Note that the surface plasma frequency 2.61 eV observed in the present data lies about 0.1 eV below the value detected in Refs.

4 and 5. This difference seems to be related to the different preparation techniques. Great care must therefore be taken when comparing the loss frequencies observed by different groups.

[38] The calculated TDLDA spectra of Refs. 20 and 26 are in excellent agreement. We recall, however, that the theoretical frequencies in Ref. 20 were shifted down by 0.36 eV to account for core polarization. Thus, the lower peak in the loss spectrum for $c=2$ in Fig. 3 of Ref. 20 corresponds to the mode $\omega_m(0) \rightarrow \omega_s(q_\parallel)$, while the upper peak is associated with $\omega_p(0) \rightarrow \omega_m(q_\parallel)$.

[39] B. N. J. Persson and E. Zaremba, Phys. Rev. B **30**, 5669 (1984).

[40] A. G. Eguiluz and J. A. Gaspar, *Springer Proceedings in Physics*, edited by M. Cardona and F. Ponce (Springer-Verlag, Heidelberg, 1991), Vol. 62, p. 23.